12-1-2009

A 236-Ghz Fe^{3+} EPR Study of Nanoparticles of the Ferromagnetic Room-Temperature Semiconductor $Sn_{1-x}Fe_xO_2$ ($x = 0.005$)

Sushil K. Misra
Concordia University

S. I. Andronenko
Concordia University

Alex Punnoose
Boise State University

Dmitry Tipikin
Cornell University

J. H. Freed
Cornell University

 DOI: 10.1007/s00723-009-0024-4

A 236-Ghz Fe^{3+} EPR Study of Nanoparticles of the Ferromagnetic Room-Temperature Semiconductor $Sn_{1-x}Fe_xO_2$ (x = 0.005)

Sushil K. Misra
Concordia University

A. Punnoose
Boise State University

S. I. Andronenko
Concordia University

Dmitry Tipikin
Cornell University

J. H. Freed
Cornell University

Abstract High-frequency (236 GHz) electron paramagnetic resonance (EPR) studies of Fe^{3+} ions at 255 K are reported in a $Sn_{1-x}Fe_xO_2$ powder with x = 0.005, which is a ferromagnetic semiconductor at room temperature. The observed EPR spectrum can be simulated reasonably well as the overlap of spectra due to four magnetically inequivalent high-spin (HS) Fe^{3+} ions (S = 5/2). The spectrum intensity is calculated, using the overlap I(BL) + (I(HS1) + I(HS2) + I(HS3) + I(HS4)) x $e^{-0.00001xB}$, where B is the magnetic field intensity in Gauss, I represents the intensity of an EPR line (HS1, HS2, HS3, HS4), and BL stands for the base line (the exponential factor, as found by fitting to the experimental spectrum, is related to the Boltzmann population distribution of energy levels at 255 K, which is the temperature of the sample in the spectrometer). These high-frequency EPR results are significantly different from those at X-band. The large values of the zero-field splitting parameter (D) observed here for the four centers at the high frequency of 236 GHz are beyond the capability of X-band, which can only record spectra of ions only with much smaller D values than those reported here.

1 Introduction

Tin dioxide (SnO_2) is an attractive system for a wide variety of practical applications [1–6], being a chemically stable transparent oxide semiconductor with a band gap of ~3.6 eV. It has been shown that Fe doping produces ferromagnetism in SnO_2 [7], thus making it a promising ferromagnetic semiconductor at room temperature. This material, therefore, has the potential for use in spintronic devices such as spin transistors, spin-LEDs, very high-density non-volatile semiconductor memory and optical emitters with polarized output [8–11], in which both the spin and charge of the particles play important roles. It is believed that oxygen vacancies and substitutional incorporation are important to produce ferromagnetism in semiconductor oxides [12], doped with transition metal ions. The details of the synthesis of the sample investigated here have been described elsewhere [7]. Transmission electron microscopy [7] showed the presence of non-spherical nanoscale particles in these samples. Quantitative magnetometry measurements showed clearly that chemically synthesized $Sn_{1-x}Fe_xO_2$ powders exhibit room-temperature ferromagnetism for $x \leq 0.05$ when prepared in the 350–600˚C range, associated with a high Curie temperature, T_c, of 850 K [7]. The present paper reports a 236-GHz electron paramagnetic resonance (EPR) investigation at 255 K of the $Sn_{1-x}Fe_xO_2$ (x = 0.005) sample prepared at 600˚C to study EPR centers characterized by large zero-field splitting (ZFS), which was not possible at X-band EPR as reported by Misra et al. [13]. Apart from determining the ZFS parameters, the focus here is to understand how the Fe^{3+} ions are incorporated into the nanoparticles in the SnO_2 lattice and their interaction with the environment.

2 Results and Discussion

EPR measurements at 236 GHz were carried out at 255 K at Cornell University on a spectrometer that used an induction mode Fabry-Pérot cavity in the warm bore of the superconducting magnet dewar containing liquid helium, where the sample, with an ambient temperature of 255 K, was placed. The magnetic field can be varied from 0.0 to 9.0 T. As seen from the experimental EPR spectrum, shown in Fig. 1, there exists an overlap of four substitutionally incorporated high-spin Fe^{3+} ions with the effective spin S = 5/2, characterized by rather large ZFS. At 255 K, the

three Fe^{3+} Kramers doublets (M = ± 5/2, ±3/2, ±1/2) are still populated, so that all the allowed EPR transitions are observed with reasonable intensities. No broad ferromagnetic line due to ferromagnetically coupled Fe^{3+} ions was observed here, because of the absence of long-range ordering of nanoparticles constituting the sample.

The spin-Hamiltonian characterizing the spin-5/2 state:

$$\mathrm{H}_S = \mu_\mathrm{B}\mathbf{B}.\mathbf{g}.S + D\left[S_z^2 - S(S+1)/3\right] + E\left[S_x^2 - S_y^2\right]$$

with B, g and μ_B being the magnetic-field intensity, g-matrix and the Bohr magneton, respectively, is used to describe the EPR spectrum due to individual Fe^{3+} ions localized in substitutional or interstitial positions with defects

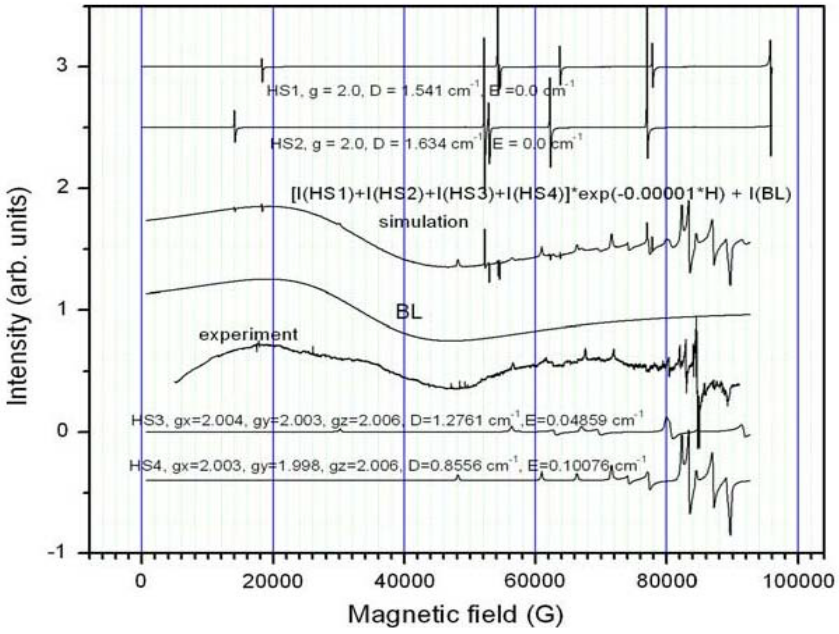

Fig. 1 Simulated and experimentally recorded first-derivative EPR absorption spectrum recorded at 236 GHz at 255 K for the 0.005% Fe^{3+}-doped SnO_2 sample prepared at 600°C. The individually simulated spectra, as well as their overlap to describe the experimental spectrum, have been displayed

around them. The spectra were simulated using Win-EPR software (Bruker). The baseline had the semblance of a spin-1/2 EPR line, described by the Zeeman interaction, μB.g.S. The overall spectrum due to the various centers, HS1, HS2, HS3, HS4 and the baseline (BL), was calculated using the overlap I(BL) + (I(HS1) + I(HS2) + I(H- S3) + I(HS4)) x exp(-0.00001 x B), where the exponential factor is related to the Boltzmann population distribution of the energy levels, I is the relative intensity of a center, and B is in Gauss. The simulated spectra are shown in Fig. 1, with the values of the spin-Hamiltonian parameters and relative intensities being listed in Table 1. The baseline seems to fit well to an S = ½ EPR spectrum. It is not identified as a ferromagnetic resonance line, because long-range order in nanoparticles is not expected, due to varying sizes of the nanoparticles in the sample. It is more characteristic of the magnetic-field sweep over a rather long range of 9 T. There is seen a good general agreement of the simulated spectrum with the experimental one. The differences in the simulated and observed line positions are due to the neglect of the fourth-order parameters in the spin Hamiltonian, whose inclusion would have certainly improved the agreement considerably. However, it would have required an exorbitant effort to vary three additional fourth-order parameters in the brute-force trial-and-error fitting carried out here. Some of the lines constituting the multitude of lines about the g = 2.0 region are due to the Fe^{3+} centers characterized by much smaller ZFS parameters (D, E) than those considered here to simulate the high-frequency spectrum, as detected in the X-band EPR spectrum [13]. No effort has been made to simulate them here; they have been addressed in [13].

Table 1 Spin-Hamiltonian parameters employed to simulate the EMR spectrum

$Fe^{3+}/Sn_{1-x}Fe_xO_2$ ($x = 0.005$)	Center/ BL	g_x	g_y	g_z	D (cm^{-1})	E (cm^{-1})	Relative intensity	Linewidth (G)
$S = 5/2$	HS1	2.0	2.0	2.0	1.541	0.0	2.0	40
	HS2	2.0	2.0	2.0	1.634	0.0	0.25	40
	HS3	2.004	2.003	2.006	1.276	0.049	0.125	180
	HS4	2.003	1.998	2.006	0.856	0.101	0.45	360
BL ($S = 1/2$)	BL	5.2	5.2	5.2			0.25	28,000

BL baseline

In SnO_2, each tin ion is octahedrally surrounded by six oxygen ions at equal distances. When a 3d impurity ion, like Fe^{3+}, substitutes for the Sn^{4+} ion, it causes an axial distortion due to the difference in size and charge. Further, this creates vacancies due to charge compensation caused by the difference in the charge of the impurity Fe^{3+} ions, which substitute for Sn^{4+} ions in SnO_2, preferably at the octahedral sites. Dusausoy et al. [14] reported that EPR spectra of four Fe^{3+} sites in single crystals of Fe^{3+}-doped SnO_2 were because of different charge compensation mechanisms, deducing that three of these four centers were due to substitutional Fe^{3+} ions, whereas the fourth Fe^{3+} center was situated at an interstitial site. In the high-frequency EPR spectrum reported here, two Fe^{3+} spectra associated with very low field lines (~14,000–18,000 G), described by rather large D parameters greater than 1.5 cm^{-1} (Table 1), are observed . This is due to the Fe^{3+} ions being situated in interstitial positions in close proximity to the surfaces of the nanoparticles in the sample, surrounded by oxygen defects, which play a leading role in determining the magnetic properties of the sample. In addition to these EPR spectra, two other EPR spectra are observed. These are due to Fe^{3+} ions being in substitutional positions with relatively smaller D parameters, although still quite large. One of them, (HS3), is close to that for the I1 Fe^{3+} EPR center reported by Dusausoy et al. [14], who assigned that center to Fe^{3+} ions in substitutional positions, where OH^- replaces O^{2-}, and the second one (HS4) is close to that for the SN Fe center reported by Dusausoy et al. [14], the site for which has not been deduced. The sign of the D parameter is chosen here to be positive in accordance with the published value [14].

At the nanoscale, the role of the nanoparticles on the surface is enhanced significantly; thus, additional effects in the EPR spectrum different from those in the bulk form are expected. The occurrence of the observed EPR lines at lower fields and changes in the linewidth are related to the anisotropy in non-spherical particles with a statistical distribution of sizes and shapes [15–17].

3 Conclusions

The EPR measurements and simulations presented here help in understanding the environments of the isolated Fe3+ ions incorporated into the SnO_2 lattice in nanoparticles at substitutional and interstitial positions. No ferromagnetic lines were observed, because a long-range ordering was not expected when there nanoparticles of varying shapes and sizes were present in the sample. The Fe^{3+} EPR spectrum reported here reveals evidence for a strong influence of surface proximity and oxygen defects. A detailed microscopic analysis of the observed spectra will require an exorbitant effort, which is not warranted over and above the main conclusions deduced here.

Acknowledgments This research was supported by NSERC, Canada (S.K. Misra); NIH/NCRR Grant P41RR016292, USA (D. Tipikin and J.H. Freed); and DMR-0449639, NSF-Idaho-EPSCoR Program, and NSF EPS-0447689 and DMR-0321051 grants (A. Punnoose).

References

1. E.J.H. Lee, C. Ribeiro, T.R. Giraldi, E. Longo, E.R. Leite, J.A. Varela, Appl. Phys. Lett. 84, 1745 (2004)
2. N. Chiodini, A. Paleari, D. DiMartino, G. Spinolo, Appl. Phys. Lett. 81, 1702 (2002)
3. P.G. Harrison, N.C. Lloyd, W. Daniell, J. Phys. Chem. B 102, 10672 (1998)
4. S.-C. Lee, J.-H. Lee, T.-S. Oh, Y.-H. Kim, Solar Energy Mater Solar Cells 75, 481 (2003)
5. S.A. Pianaro, P.R. Bueno, E. Longo, J.A. Varela, J. Mater. Sci. Lett. 14, 692 (1995)
6. E.A. Bondar, S.A. Gormin, I.V. Petrochenko, L.P. Shadrina, Opt. Spectrosc. 89, 892 (2000)
7. A. Punnoose, J. Hays, A. Thurber, M.H. Engelhard, R.K. Kukkadapu, C. Wang, V. Shutthanandan, S. Thevuthasan, Phys. Rev. B 72, 054402 (2005)
8. G.A. Prinz, Science, 282, 1660 (1998); J. Magn. Magn. Mater. 200, 57 (1999)
9. S.A. Chambers, R.F.C. Farrow, MRS Bull. 28, 729 (2003)
10. S.J. Pearton, C.R. Abernathy, M.E. Overberg, G.T. Thaler et al., J. Appl. Phys. 93, 1 (2003)
11. N. Lebedeva, P. Kuivalainen, J. Appl. Phys. 93, 9845 (2003)
12. J.M.D. Coey, A.P. Douvalis, C.B. Fitzgerald, M. Venkatesan, Appl. Phys. Lett. 84, 1332 (2004)
13. S.K. Misra, S.I. Andronenko, K.M. Reddy, J. Hays, A. Thurber, A. Punnoose, J. Appl. Phys. 101, 09H120 (2007)
14. Y. Dusausoy, R. Ruck, J.M. Gaite, Phys. Chem. Miner. 15, 300 (1988)
15. K. Nagata, A. Ishihara, J. Magn. Magn. Mater. 104–107, 1571 (1992)
16. A. Punnoose, M.S. Seehra, J. van Tol, L.C. Brunel, J. Magn. Magn. Mater. 288, 168 (2005)
17. A. Punnoose, M.S. Seehra, in EPR in the 21st Century, ed. by A. Kawamori, J. Yamauchi, H. Ohta (Elsevier Science, 2002), 162 pp